Study on the novel neutron-to-proton convertor for improving the detection efficiency of a triple GEM based fast neutron detector *

WANG Xiao-Dong(王晓冬)[1] YANG He-Run(杨贺润)[2] REN Zhong-Guo(任忠国)[3]
ZHANG Jun-Wei(张俊伟)[2] YANG Lei(杨磊)[1] ZHANG Chun-Hui(张春晖)[1]
HA Ri-Ba-La(哈日巴拉)[4] AN Lü-Xing (安旅行)[5] HU Bi-Tao(胡碧涛)[1;1)]

[1] School of Nuclear Science and Technology, Lanzhou University, Lanzhou 730000, China
[2] Institute of Modern Physics, Chinese Academy of Sciences, Lanzhou, 730000, China
[3] China Academy of Engineering Physics, Mianyang 621907, China
[4] Inner Mongolia Center for Disease Control and Prevention, Hohhot, 010031, China
[5] LWD Logging Center, China Petroleum Logging CO. LTD., Xi'an 710000, China

Abstract: A high-efficiency fast neutron detector prototype based on a triple Gas Electron Multiplier (GEM) detector, which, coupled with a novel multi-layered high-density polyethylene (HDPE) as a neutron-to-proton converter for improving the neutron detection efficiency, is introduced and tested with the Am-Be neutron source in the Institute of Modern Physics (IMP) at Lanzhou in the present work. First, the developed triple GEM detector is tested by measuring its effective gain and energy resolution with ^{55}Fe X-ray source to ensure that it has a good performance. The effective gain and obtained energy resolution is 5.0×10^4 and around 19.2%, respectively. Secondly, the novel multi-layered HDPE converter is coupled with the cathode of the triple GEM detector making it a high-efficiency fast neutron detector. Its effective neutron response is four times higher than that of the traditional single-layered conversion technique when the converter layer number is 38.

Key words: Gas Electron Multiplier, deposited energy, Am-Be neutron source, neutron detection efficiency, fast neutron detector

PACS: 29.40.Gx, 29.40.Cs, 07.05.Tp **DOI:** 10.1088/1674-1137/39/2/026001

1 Introduction

The original intention of the Gas Electron Multiplier (GEM) detector was to detect charged particles, due to its excellent performances [1, 2], such as withstanding electrical discharge without damage, good position resolution, high effective gain and an adjustable active region and so on. It became a neutron detector by coupling with a conversion layer, which represents a kind of platform in both thermal and fast neutron detection fields [3–6]. Two very common neutron interactions used for detecting the thermal neutron are the reactions of

$$n+{}^6\mathrm{Li}\rightarrow{}^4\mathrm{He}+{}^3\mathrm{H}+4.79\ \mathrm{MeV} \text{ and } n+{}^{10}\mathrm{B}\rightarrow {}^7\mathrm{Li}^*+{}^4\mathrm{He}$$

$$\rightarrow{}^4\mathrm{He}+{}^7\mathrm{Li}+\gamma(0.48\ \mathrm{MeV})+2.31\ \mathrm{MeV}(93\%)$$
$$\rightarrow{}^7\mathrm{Li}+{}^4\mathrm{He}+2.79\ \mathrm{MeV}\qquad(7\%)\ [7].$$

However, low atomic number materials, such as polyethylene and acrylonitrile (C_3H_3N), usually have low cost and relatively higher elastic scattering cross sections for detecting the fast neutrons. In addition, H(n, n$'$)p process among the fast neutron interactions with hydrogen-rich materials is dominant. Regardless of the thermal neutron or the fast neutron, the charged particles emitted as a result of neutron interaction with converters, such as ^{10}B, ^{6}Li and hydrogen, can be easily detected by the triple GEM detector, in which the charged particles create detectable signals by ionizing gas atoms and finally are collected by a read-out anode of the detector.

Usually, the detection efficiency of fast neutrons is very low, less than 0.1% [8, 9] and therefore how to improve it is also a very important issue elaborated in this work. The high-efficiency fast neutron detector developed and tested in the present work consists of a triple GEM detector and a converter. The triple GEM detector is constructed and tested with ^{55}Fe source first. Then, a single-layered HDPE converter is coupled with the triple GEM detector to make it work as a neutron detector. At last, to improve the neutron detection efficiency, a novel multi-layered HDPE as the neutron-to-proton converter

Received 14 March 2014
* Supported by National Natural Science Foundation of China (11135002, 11305232, 11175076)
1) E-mail: hubt@lzu.edu.cn

is installed in the triple GEM detector and tested by measuring neutron deposited energy spectrum with Am-Be source as in [5, 10].

2 Experimental setup for a high-efficiency fast neutron detector

The high-efficiency fast neutron detector is a four-stage parallel plate avalanche chamber and works in a proportional mode as shown in Fig. 1. It consists of a cathode plane, three GEMs, and a read-out anode (printed circuit board (PCB)). The 2 μm thick Al foil is coated on the multi-layered HDPE converter as the cathode. According to the calculation result and recently manufactured condition, each converter layer is set to 1 mm thick. As shown in Fig. 2, two different conversion structures are used for testing in this work, including a traditional single layer marked as A and novel multi-layered conversion structures marked B and C, (the layer number of B mode and C mode is 21 and 38, respectively).

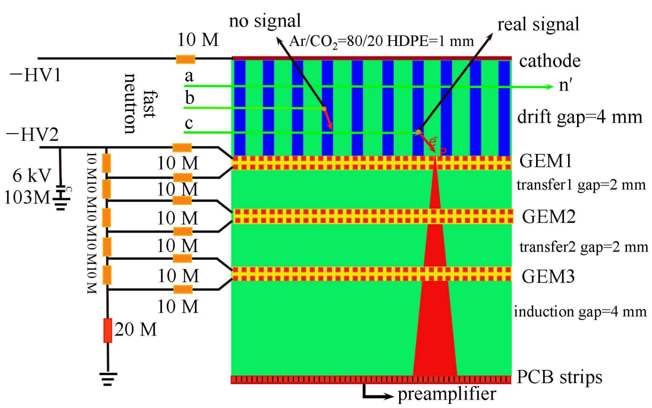

Fig. 1. (color online) Experimental principal scheme of the high-efficiency fast neutron detector. The a, b and c represents three different physics processes which are: (a) a neutron directly goes through the converter without any interaction; (b) a recoiling proton knocked out by a neutron′s elastic scattering with the converter does not yet have enough energy to escape the converter and terminates in the converter; (c) a neutron knocks out an energetic recoiling proton enabled to escape the converter, ionize the gas atoms and produce an effective signal in the detector. The yellow blocks represent the resistors. Other information is described in the scheme.

The detector has a volume of 290 mm×290 mm×56 mm, a square active area of 100 mm×100 mm, a 4 mm wide drift gap, where the process of primary ionization happens, two 2 mm wide transfer gaps, where all electrons transfer toward the induction gap, and a 4 mm wide induction gap, where all avalanche electrons are induced as the detectable signal to the read-out PCB (printed circuit board) anode. The anode plane is made of one-dimensional parallel strips with standard printed circuit board technology. All read-out strips (496) are shorted together for acquiring an integrated anode signal and are connected to the electric readout system. The width of a strip is 80 μm and the interval between two strips is 110 μm.

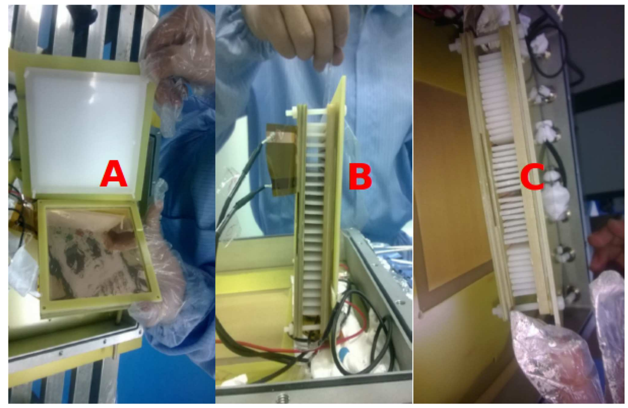

Fig. 2. (color online) Two different conversion structures are employed in the present work, including traditional single-layered and novel multi-layered HDPE.

The detector is operated based on a continuously flushed Ar/CO_2 gas mixture (80/20 percentage in volume). The bias voltage is delivered to each electrode through a passive resistor divider by CAEN module N472. An additional 10 MΩ protection resistor connected with a GEM electrode is placed in series for releasing discharges. To obtain the pulse height spectrum, the signal is read out by an electronic system comprised of preamplifier Ortec 142PC, amplifier CAEN N968, Ortec CF8000, Ortec GG8000 and Philip ADC 7164 and other CAMAC modules.

The detector is tested with the Am-Be source in the IMP of Lanzhou.

3 The basic performances of a triple GEM detector

3.1 Effective gain

Effective gain is a very important character for the GEM detector. Since it generally impacts the energy resolution, the time resolution and position resolution, three common methods are often employed to improve effective gain in principle. First, by improving the drift field, the ionization electrons can obtain enough kinetic energy to avoid the recombination effect, and go through the GEM hole to produce an avalanche. Secondly, by improving the high voltage across the GEM electrodes, the electronic field inside the GEM hole becomes stronger and the electrons passing through it can obtain enough kinetic energy to trigger further secondary ionization. Thirdly, a higher induction field can drag the avalanche electrons out of the GEM holes more easily to produce detectable signals. In the present work, the effective gain of the triple GEM detector in different drift E_{D} and the high voltage across the three GEM electrodes $V_{\mathrm{TGEM}}(V_{\mathrm{gem1}}+V_{\mathrm{gem2}}+V_{\mathrm{gem3}})$ is studied, respectively. ^{55}Fe X-ray source is collimated by an iron collimator with a 2 mm hole on the top of the detector.

The effective gain as a function of E_{D} is shown in Fig. 3. With the increase of the E_{D}, the effective gain has a harsh growth and reaches a saturation plateau when the E_{D} is between 1–2.4 kV/cm. When the drift field is higher than 2.4 kV/cm, the ionization electrons hit the copper of the GEM foil instead of drifting out of the GEM holes, which results in the effective gain declining aggressively.

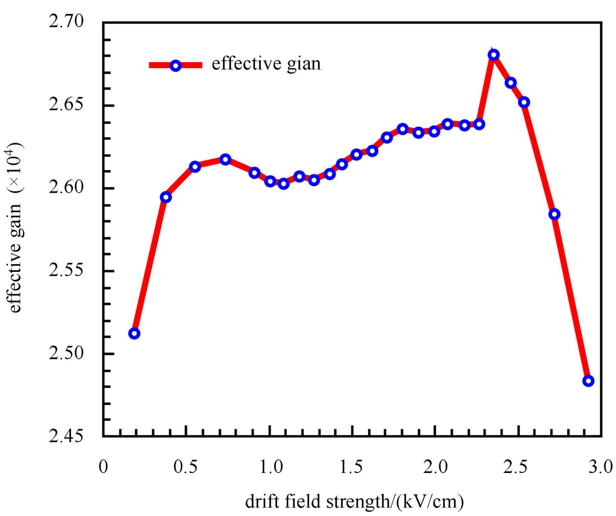

Fig. 3. (color online) Effective gain of the triple GEM detector as a function of E_{D} with ^{55}Fe 5.9 keV X-ray, V_{TGEM}=991 V and induction field is 2 kV/cm.

As shown in Fig. 4 the effective gain of the detector increases in a good exponential way as the V_{TGEM} increases. When the V_{TGEM} is up to 1017 V, the effective gain reaches a maximum value of 5.0×10^4, where the preamplifier 142 PC appears saturated in this work.

3.2 The energy resolution

The energy resolution of the triple GEM detector is tested with ^{55}Fe 5.9 keV X-ray. Fig. 5 shows the energy spectrum under conditions of E_{D}=2 kV/cm, V_{TGEM}=1017 V and E_{I}=2 kV/cm. The detector is operated at the effective gain of 5.0×10^4. The energy resolution is about 19.2%. The full photo-electron peak of ^{55}Fe and the escape peak of the argon atom is distinguished completely. The ratio of the two peaks is 1.98, which demonstrates that the detection system has a good energy linearity relationship. As shown in Fig. 6, the energy resolution is better when V_{TGEM} increases; when

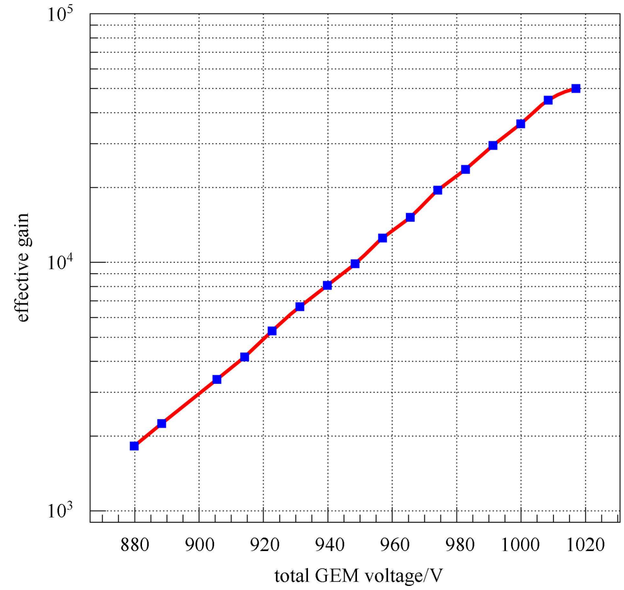

Fig. 4. (color online) Effective gain of the triple GEM detector as a function of V_{TGEM} with ^{55}Fe 5.9 keV X-ray irradiation under conditions of electric field strength of E_{D}=2 kV/cm and E_{I}=2 kV/cm; Ar/CO_2=80/20, room temperature.

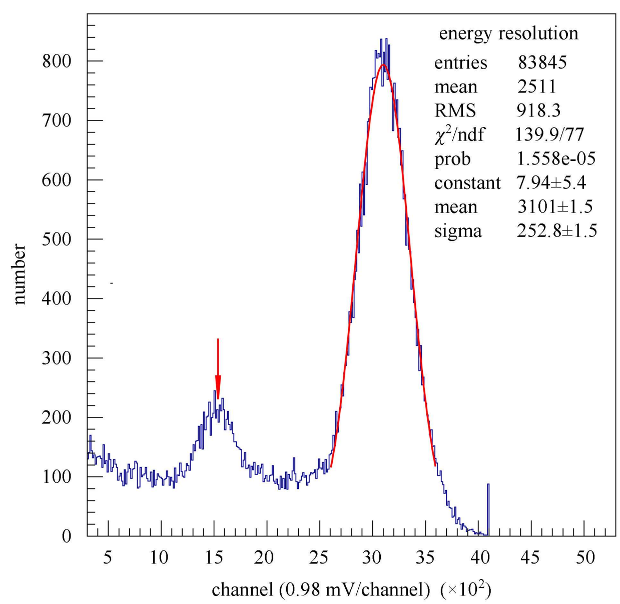

Fig. 5. (color online) Energy spectrum of ^{55}Fe 5.9 keV X-ray detected with triple GEM detector with V_{TGEM}=1017 V, E_{D}=2 kV/cm, E_{I}=2 kV/cm, Ar/CO_2=80/20, room temperature.

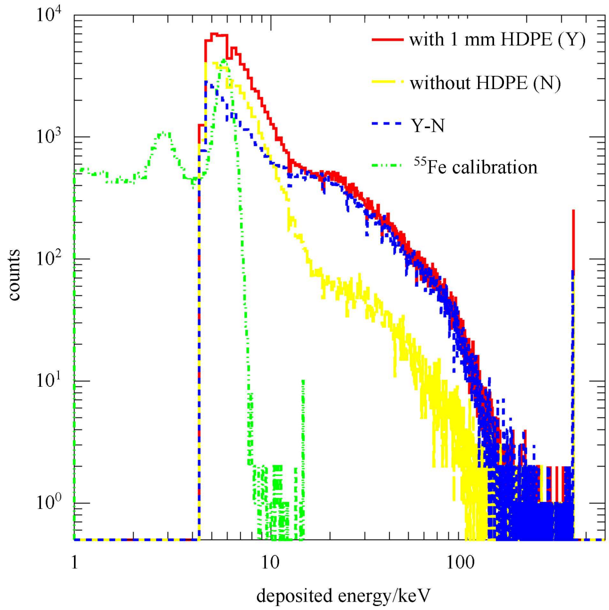

Fig. 6. (color online) Energy spectrum measured with Am-Be neutron. The sample Y (solid line) and N (long dash line) represent the total energy spectrum and background spectrum, respectively. Y and N are obtained with or without the 1 mm HDPE conversion layer under the same conditions. The sample (Y-N) represents an entire neutron energy deposition. The line of long dash double points represents ^{55}Fe X-ray energy spectrum to show the detector working status.

the V_{TGEM} is up to 1017 V, the energy resolution reaches the best value of 19.2% in this test.

4 The results of the high-efficiency fast neutron detector based on triple GEM

The single-layered HDPE marked as A in Fig. 2 is employed as a traditional technology. In this test, the effective gain of the triple GEM detector is set to 2000 in order to reduce the sensitivity to gamma. The threshold of the CF8000 is set to 21 mV for deceasing the system noise. The neutron response spectrum Y and N were under the same conditions except the converter. Y is with 1 mm HDPE, whereas N is without it. The experimental results are shown in Fig. 7. In the spectrum (Y-N), three different components can be distinguished clearly. Similar results have been found in simulation and experiment [11, 12].

(a) The lower than 18 keV part is considered to be from the activation photons, which librate electrons by Compton scattering to deposit their energies in the detector and contribute to the lower energy part of the neutron spectrum.

(b) The higher than 18 keV part is regarded as the real neutron response signals. The charged particles coming from the neutron converter of the HDPE and the GEM Kapton deposit higher energies than the Compton electrons do. This part is called the neutron conversion region in the energy spectrum, which demonstrates the real response events of the detector to neutrons.

(c) The peak around 320 keV is due to the saturation of the employed 142 PC preamplifier.

As a comparison with the single-layered traditional

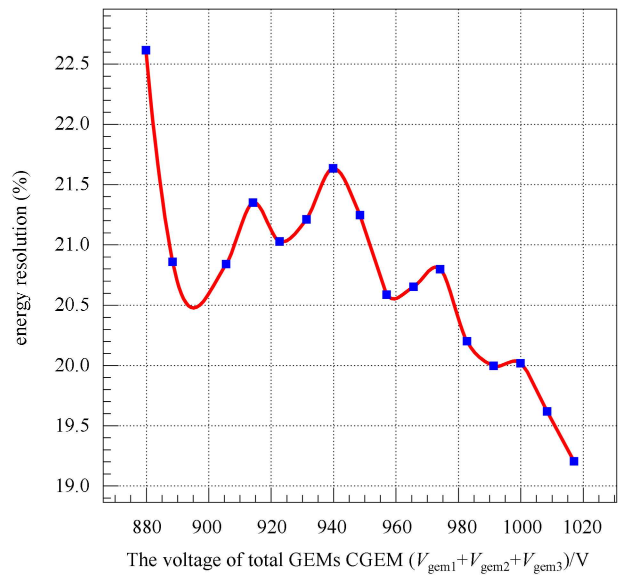

Fig. 7. (color online) Energy resolution of the triple GEM detector as a function of V_{TGEM} with ^{55}Fe 5.9 keV X-ray, drift and induction field is 2 kV/cm and 2 kV/cm, respectively.

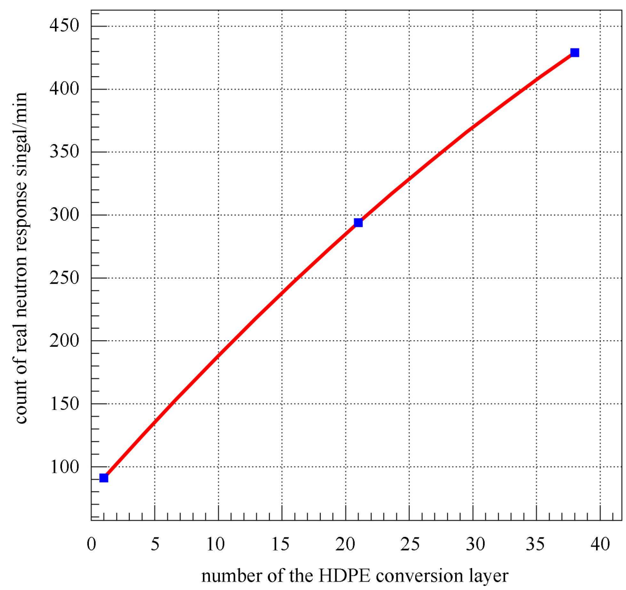

Fig. 8. (color online) The count of real neutron response events as a function of the number of converter layers; the number of the converter layer is 1, 21 and 38 layers, respectively.

conversion method, the novel multi-layered HDPE converter is tested, too. The layer number of the converter is designed to be 21 and 38 respectively and marked as B and C in Fig. 2. The multi-layered conversion detector is measured with the same conditions as that of the single-layered. The value of the real neutron response event rate is subtracted from the energy spectrum for comparison with the traditional conversion technique. As shown in Fig. 8, the results show that the relative detection efficiency of the novel multi-layered neutron detector is about four times higher than that of the traditional method when the converter layer number is 38.

5 Conclusions and discussions

Basic performances of the triple GEM detector are studied by measuring effective gain and energy resolution with ^{55}Fe X-ray source. The experiment results confirm that the triple GEM detector has a high effective gain about 5.0×10^4 and a good energy resolution around 19.2% under a lower safe high voltage. The neutron GEM-based detectors with single-layered and multi-layered HDPE converters are studied. By comparing with the count of the real neutron response event rate, the multi-layered converter technique is higher than that of the traditional signal-layered one. In other words, the multi-layered neutron conversion technique can greatly improve neutron detection efficiency in practical applications, which opens a new method to detect the neutron in the future.

For the novel multi-layered conversion technique, due to limitations of the current production technique and mechanical constraints, it is hard to ensure converter surface without burr, which results in HDPE charging up and further leads to distortion of the electric field in drift volume. This affects the efficiency in collecting and focusing the ionization electrons to the GEM holes and thus significantly decreases the total effective events. In addition, because the neutron source used in this test is not a mono-energy such as a D-T neutron source, only the relative detection efficiency is presented rather than the absolute detection efficiency.

As discussed above, there are two important things that should be done in the next work. They are that the multi-layered converter should be manufactured by 3D print technology to improve the surface quality of the converter, and a mono-energy neutron source should be employed to finally figure out the absolute detection efficiency.

We are grateful to researcher DUAN Li-Min, associate researcher Hu Rong-Jiang and Dr LU Chen-Gui for their helpful discussions and support in the Institute of Modern Physics, Chinese Academy of Sciences.

References

1 Fabio S. Nucl. Instrum. Methods A, 1997, **386**: 531–534
2 Bressan A, De Oliveira R, Gandi A et al. Nucl. Instrum. Methods A, 1999, **425**: 254–261
3 Ohshita H, Uno S, Otomo T, Koike T et al. Nucl. Instrum. Methods A, 2010, **623**: 126–128
4 WANG Y F, SUN Z J, ZHOU J R et al. Science China Physics, Mechanics & Astronomy, 2013, **56**: 1897–1902
5 WANG X D, ZHANG Y L, ZHANG C H et al. Science China Physics, Mechanics & Astronomy, 2013, **56**: 1740–1744
6 ZHOU Jian-Rong, SUN Zhi-Jia, LIU Ben et al. CPC (HEP & NP), 2011, **35**(7): 668–674
7 Oed A. Nucl. Instrum. Methods A, 2004, **525**: 62–68
8 ZHANG Y, ZHANG X D, WANG W X et al. CPC (HEP & NP), 2009, **33**(1): 42–46
9 WANG Y, CHENG J P, LI Y J et al. CPC (HEP & NP), 2010, **34**(1): 88–91
10 Cortesi M, Zboray R, Adams R et al. JINST, 2012, **7**: C02056
11 Croci G, Alfonsi M, Ropelewski L et al. Nucl. Instrum. Methods A, 2013, **712**: 108–112
12 Esposito B, Marocco D, Villari R et al. Nucl., 2014, **741**: 196–204